



OPEN

dTrmt10A impacts Hsp70 chaperone m⁶A levels and the stress response in the *Drosophila* brain

Alexandra E. Perlegos^{1,2}, Xiuming Quan², Kirby M. Donnelly², Hui Shen³, Emily J. Shields^{4,5}, Heidi Elashal^{6,7}, Kathy Fange Liu^{6,7} & Nancy M. Bonini^{1,2}✉

Chronic cellular stress has a profound impact on the brain, leading to degeneration and accelerated aging. Recent work has revealed the vital role of RNA modifications, and the proteins responsible for regulating them, in the stress response. In our study, we defined the role of *CG14618/dTrmt10A*, the *Drosophila* counterpart of human *TRMT10A* a *N*¹-methylguanosine methyltransferase, on m⁶A regulation and heat stress resilience in the *Drosophila* brain. By m⁶A-IP RNA sequencing on *Drosophila* head tissue, we demonstrated that manipulating *dTrmt10A* levels indirectly regulates m⁶A levels on polyA + RNA. *dTrmt10A* exerted its influence on m⁶A levels on transcripts enriched for neuronal signaling and heat stress pathways, similar to the m⁶A methyltransferase *Mettl3*. Intriguingly, its impact primarily targeted 3' UTR m⁶A, setting it apart from the majority of *Drosophila* m⁶A-modified transcripts which display 5' UTR enrichment. Upregulation of *dTrmt10A* led to increased resilience to acute heat stress, decreased m⁶A modification on heat shock chaperones, and coincided with decreased decay of chaperone transcripts and increased translation of chaperone proteins. Overall, these findings establish a potential mechanism by which *dTrmt10A* regulates the acute brain stress response through m⁶A modification.

RNA modifications are emerging as a critical layer of gene expression that impact various biological functions in the brain, such as learning and memory, neurogenesis, and developmental transitions^{1–7}. Mutations in methylation complex proteins and dysregulation in RNA modification can lead to severe developmental defects, compromised cellular stress responses, and tumorigenesis^{8–10}. *TRMT10A* is an S-adenosylmethionine-dependent methyltransferase that installs the RNA modification *N*¹-methylguanosine (m¹G) on tRNAs at the ninth position; it is the only known methyltransferase that installs m¹G on human tRNA^{11,12}. tRNAs are among the most heavily modified classes of RNA and these modifications are critical for the stability and translation functionality of tRNAs^{11,12}. Mutations of *TRMT10A* in humans have been linked to primary microcephaly, mild intellectual disability, young onset diabetes, and apoptosis in pancreatic cells^{13–17}. However, the mechanisms by which genetic mutations in *TRMT10A* cause these phenotypes are not well understood.

*N*⁶-methyladenosine (m⁶A) is the most abundant internal modification of eukaryotic mRNA^{1,18,19}. It is deposited co-transcriptionally by a methyltransferase, *METTL3*, with the help of additional structural proteins. m⁶A levels are dynamically regulated by writer, reader, and eraser proteins^{8,19}. The m⁶A modification of mRNA provides a critical layer of regulation in neuronal responses to cellular stress and disease^{20–22}. Interaction of m⁶A transcripts with reader proteins can dictate downstream processing, including splicing, decay, and translation^{23–26}. *TRMT10A* has been shown to interact with the m⁶A RNA demethylase FTO and promote its demethylase activity in HEK293T cells²⁷. Loss of *TRMT10A* increases m⁶A methylation on FTO RNA targets in cultured cells²⁷. m⁶A levels are enriched in brain tissue of human, mice, and *Drosophila*, and mark transcripts involved in synaptic

¹Neuroscience Graduate Group, Perelman School of Medicine, University of Pennsylvania, Philadelphia, PA 19104, USA. ²Department of Biology, University of Pennsylvania, Philadelphia, PA 19104, USA. ³School of Life Science and Technology, China Pharmaceutical University, Nanjing 210009, Jiangsu, China. ⁴Epigenetics Institute, Perelman School of Medicine, University of Pennsylvania, Philadelphia, PA, USA. ⁵Department of Cell and Developmental Biology, Perelman School of Medicine, University of Pennsylvania, Philadelphia, PA, USA. ⁶Department of Biochemistry and Biophysics, Perelman School of Medicine, University of Pennsylvania, Philadelphia, PA 19104, USA. ⁷Graduate Group in Biochemistry and Molecular Biophysics, Perelman School of Medicine, University of Pennsylvania, Philadelphia, PA 19104, USA. ✉email: nbonini@sas.upenn.edu

growth, axon guidance and signaling^{22,28–30}. m⁶A reader proteins, or YTH domain-containing proteins, are known for their ability to promote translation and decay of m⁶A-modified RNAs^{7,31–33}. One of their characterized functions is the ability to regulate cortical neurogenesis through precise decay of neuronal m⁶A transcripts during developmental transitions in mouse and human cells^{30,33}.

During cellular stress, the role of m⁶A modifications becomes amplified with increased methylation dynamically regulating RNAs for rapid degradation and/or selective translation^{20,28,34–37}. During UV DNA damage stress, m⁶A methylation functions in recruitment of DNA damage machinery³⁸, and during heat stress transcripts become marked for decay and translation in in vitro human cell culture models^{39–41}. Neurons are critically vulnerable to prolonged stress and degenerative disease. Heat shock protein chaperones (HSPs) are known to protect neuronal cells against protein misfolding, accumulation and aggregation, but HSPs are dysregulated during aging and disease⁴².

Drosophila is a powerful genetic model system that has pioneered numerous fundamental discoveries in brain development and disease. Homologous m⁶A methyltransferase complex components are enriched in the *Drosophila* central nervous system (CNS), making the fly an ideal system for understanding m⁶A modification in brain functions¹⁹. In *Drosophila*, m⁶A is implicated in female specific alternative splicing of the master sex determination regulatory gene *Sex-lethal* (*Sxl*)^{23,43,44}. Additionally, the *Drosophila* cytoplasmic m⁶A reader protein Ythdf regulates axonal overgrowth through interactions with Fmr1, the fly homolog of Fragile X mental retardation protein, and together they inhibit translation of m⁶A modified targets of Fmr1⁴⁵. Furthermore, there is no identified homologous m⁶A demethylase in *Drosophila*.

Here, we investigate the fly homolog of *TRMT10A*, *CG14618* (which we now refer to as *dTrmt10A*), to uncover its regulation of m⁶A levels and the stress response in the *Drosophila* brain. The role of *TRMT10A/dTrmt10A* and its effects on m⁶A levels have not been studied in vivo. Our m⁶A-IP sequencing results indicate that *dTrmt10A* impacts m⁶A on signaling transcripts, and alters m⁶A on key heat stress chaperone transcripts^{3,46}. We find that upregulation of *dTrmt10A* acts similarly to loss of m⁶A methyltransferase *Mettl3* in the *Drosophila* brain, and highlights m⁶A peaks in the 3'UTR of transcripts. These findings indicate that *dTrmt10A* modulates m⁶A in *Drosophila* and plays a critical role in regulating the stress response of the brain.

Results

m⁶A is enriched in the brain and *dTrmt10A* knockdown increases m⁶A levels on Hsp70 transcripts.

The *Drosophila* gene *CG14618* is the predicted homolog of the human *TRMT10A* methyltransferase. Using Clustal Omega, human *TRMT10A* and *Drosophila* *CG14618* share 36.8% amino acid sequence identity, with 100% conservation in the m¹G catalytic domain "YVIGGLVDHNNH" (Fig. 1A). We refer to *CG14618* as *Drosophila Trmt10A* (*dTrmt10A*) from here on. Knockdown of *dTrmt10A* in vivo produced viable offspring. Using liquid chromatography-tandem mass spectrometry (LC-MS/MS), we confirmed significant m¹G level reduction in *dTrmt10A* RNAi brains (small RNA fraction < 200 nucleotides), compared to control brains (Fig. 1B). *dTrmt10A* mRNA levels in head tissue were significantly reduced by RT-qPCR and RNA-seq analysis (Fig. 1C,D and Supplementary Data 1).

Given that *TRMT10A* interacts with FTO in mammalian cells²⁷, we conducted m⁶A-IP sequencing analysis of polyA + RNA from *Drosophila* heads expressing *dTrmt10A* RNAi. IP sequencing confirmed that m⁶A is enriched in the 5'UTR of transcripts in *Drosophila* heads, consistent with our and others previous work^{3,46}. Enrichment of m⁶A in the 5'UTR is unique to *Drosophila*, as mammalian m⁶A is primarily located in the 3'UTR²⁸. Global metagenome analysis highlighted that *dTrmt10A* knockdown increased m⁶A levels in the 5'UTR of transcripts, and unexpectedly also showed increased m⁶A in the 3'UTR of a subset of transcripts (Fig. 2A).

To determine which transcripts showed significant differential methylation between control and *dTrmt10A* knockdown conditions, we utilized RADAR analysis with a beta-threshold of 0.5. Using these parameters, only transcripts from a single gene showed a significant increase in m⁶A. These transcripts encode the heat shock chaperone protein Hsp70 (Fig. 2B). We were particularly intrigued by this finding as there are normally low levels of m⁶A in the 5'UTR on *Hsp70* transcripts at baseline, and m⁶A signal is lost upon acute heat stress in the *Drosophila* brain⁴⁶. Previously, we found that knockdown of m⁶A methyltransferase *Mettl3* showed increased RNA and protein levels of Hsp70 at baseline along with increased heat stress resilience⁴⁶. We asked if an opposite effect occurred with knockdown of *dTrmt10A*. In *dTrmt10A* RNAi brains, RNA and protein levels of Hsp70 were reduced (Fig. 2C,D). Additionally, *dTrmt10A* RNAi animals exhibited increased stress sensitivity (Fig. 2E). These data indicate that *dTrmt10A* RNAi exerts contrasting effects on Hsp70 RNA, protein, and m⁶A levels compared to *Mettl3* RNAi.

To visualize global changes in m⁶A, regardless of peak calling threshold, we generated a scatterplot of m⁶A-IP reads divided by input read coverage in the 5'UTR for *Mettl3*-dependent m⁶A transcripts. Upon *dTrmt10A* knockdown, we observed a global shift towards increased levels of m⁶A in the 5'UTR of transcripts (Fig. 2F), similar to the global metagenome analysis (Fig. 2A). We observed a slight increase of 5'UTR m⁶A on other chaperones such as Heat shock chaperone 40 (*DnaJ-1*) (Fig. 2G), but no changes comparable to the increase on *Hsp70* 5'UTR. These findings highlight the regulation of *Hsp70* transcripts by the m⁶A machinery, and indicate it as key target of *dTrmt10A*.

To analyze the impact of m⁶A on RNA levels with *dTrmt10A* manipulation, we employed an ex-vivo brain RNA decay assay. Reduced m⁶A by *Mettl3* RNAi lead to higher steady state levels and decreased rate of decay of m⁶A transcripts⁴⁶. We examined the relative levels of RNA remaining in *dTrmt10A* RNAi brain samples after 4 h, in the presence of actinomycin D. *dTrmt10A* RNAi brains (with increased m⁶A) had increased decay of *Hsp70* RNA transcript levels compared to control brains, and no significant difference of *RpL32*, which is a control

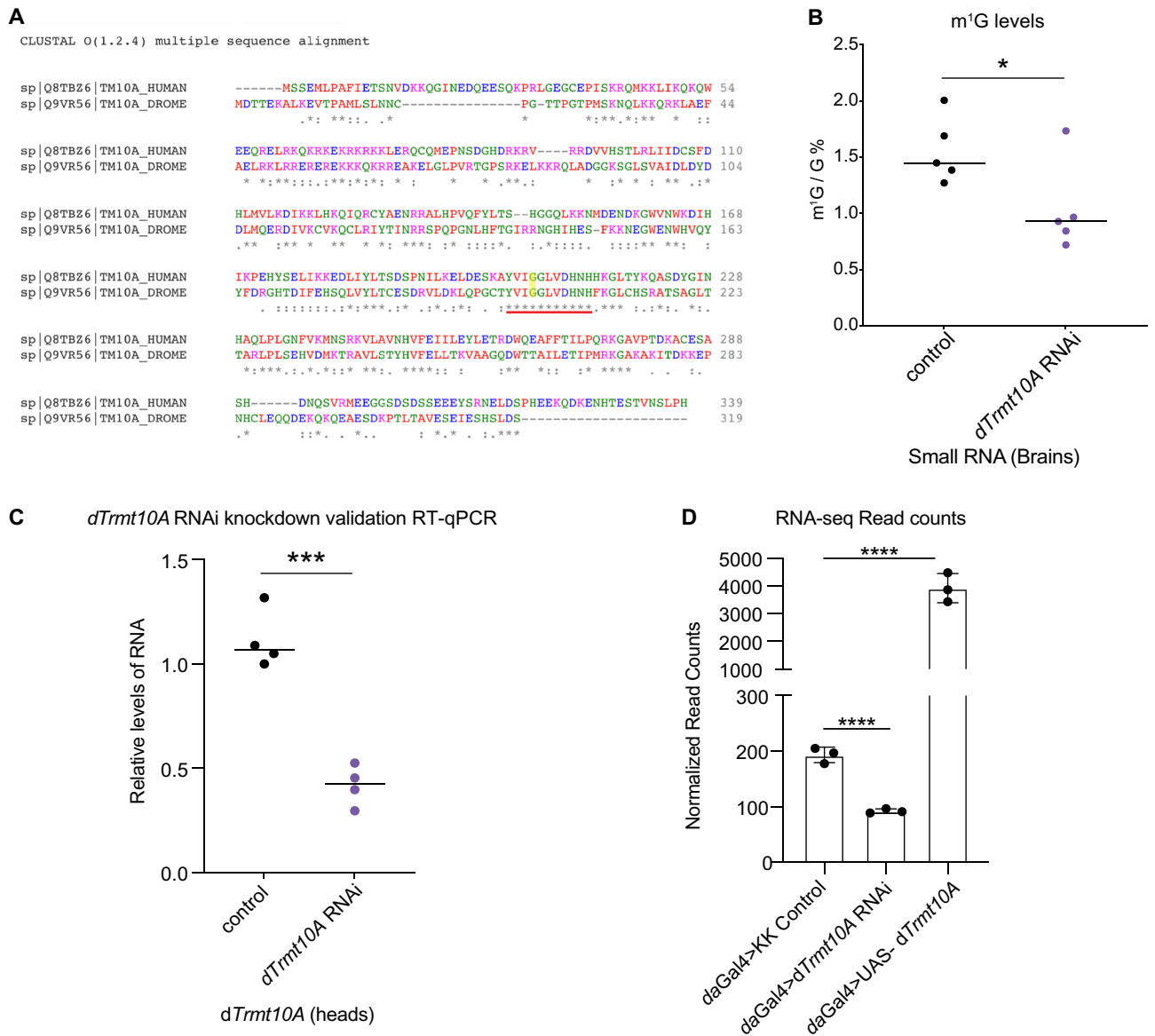


Figure 1. Impact of the *Drosophila* homolog of TRMT10A on m¹G and m⁶A levels. **(A)** Alignment of Human TRMT10A and *Drosophila* *dTrmt10A*/CG14618 by Clustal Omega multiple sequence comparison. Asterisk * indicates fully conserved residues, a colon indicates conservation of strongly similar properties, and period indicates conservation of weakly similar properties. Protein alignment shows overall 36% conservation between *Drosophila* and human domain. Red line indicates conserved m¹G catalytic domain, and G206R mutation highlighted in yellow indicates catalytic mutant. **(B)** LC-MS/MS analysis of m¹G/G% levels from brain small RNA in basal conditions, in control vs *dTrmt10A* RNAi, *n* = 5 biological replicates, 30 brains per replicate. Data are presented as mean, t-test **p* < 0.05. **(C)** RNA levels of *dTrmt10A* were assessed by RT-qPCR. *daGal4* > UAS-KK control (Vienna 60100); *daGal4* > UAS-*dTrmt10A* RNAi (Vienna 100720); *n* = 3 biological replicates, 15 brains per replicate. Data are presented as mean, t-test, ****p* < 0.001. **(D)** RNA levels of *dTrmt10A* determined from RNA-sequencing *Drosophila* head tissue, normalized read counts and statistical analysis done by Deseq2. See Supplementary Data 1 for details of fly genotypes in all figures.

non-m⁶A modified transcript (Fig. 2H). These data suggest that *dTrmt10A* influences the stability of Hsp70 transcripts and overall protein and RNA levels, likely by modulating their m⁶A levels.

Upregulation of *dTrmt10A* decreases m⁶A levels and enhances the stress response of the brain.

Studies investigating the role of TRMT10A in cultured cells have focused on mutations or gene downregulation^{17,27}. To determine whether upregulation of *dTrmt10A* could also regulate m⁶A levels, we utilized a FLAG-HA C-terminal tagged ORF clone of *dTrmt10A* to generate animals that upregulate *dTrmt10A* (Supplementary Fig. 1A). Upregulation of *dTrmt10A* showed no global effect on m¹G levels, likely due to the saturation of m¹G levels on tRNAs (Supplementary Fig. 1B). m⁶A-IP sequencing analysis conducted on *Drosophila* heads with *dTrmt10A* upregulation revealed a striking reduction in m⁶A levels (Fig. 3A). A closer look at heat stress

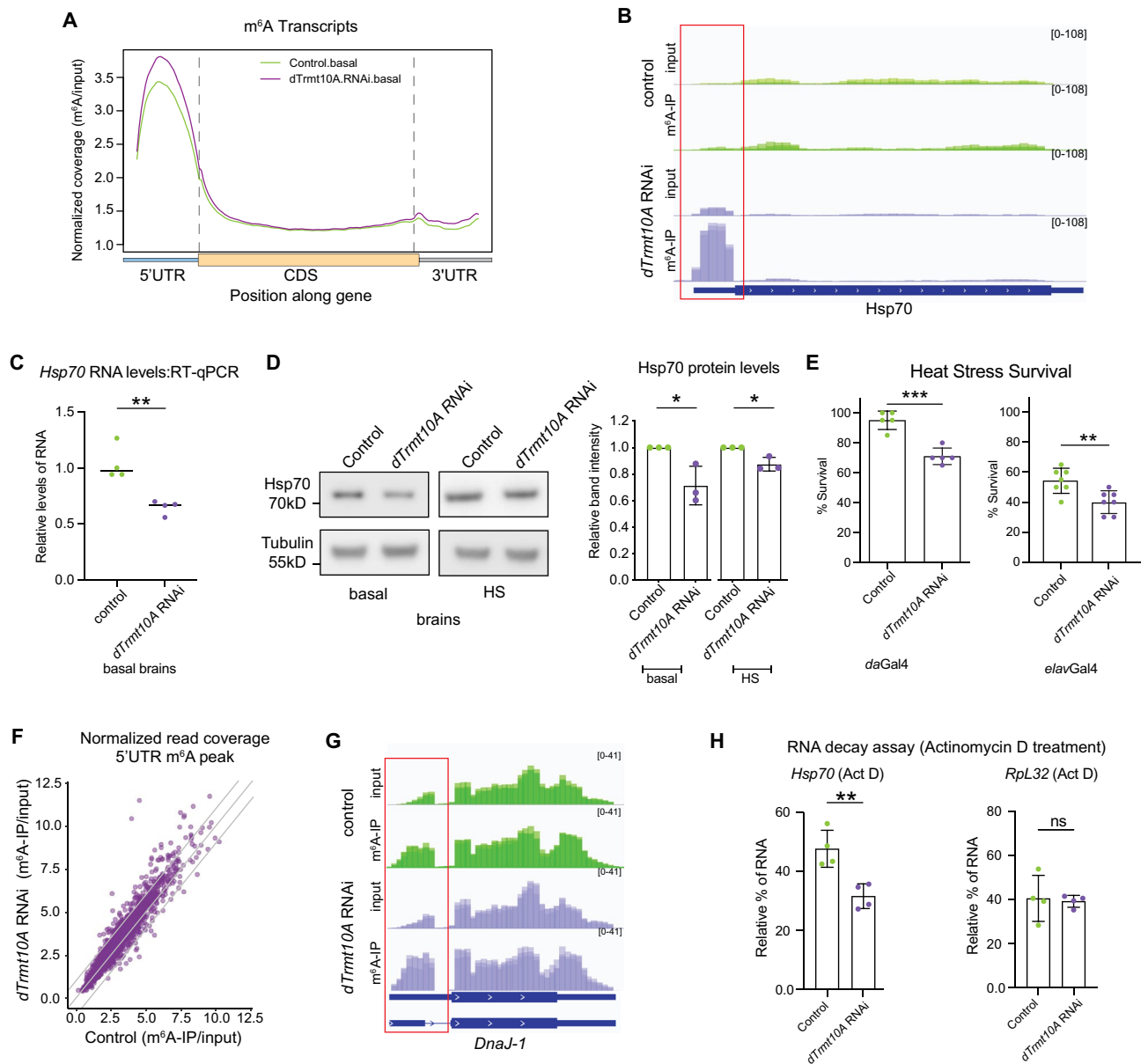


Figure 2. *dTrmt10A* knockdown increases m⁶A on the 5'UTR of *Hsp70* transcripts. **(A)** Normalized read coverage plot of m⁶A-IP/input on polyA⁺ transcripts in the 5'UTR, CDS, and 3'UTR of m⁶A genes. m⁶A-IP sequencing in basal conditions from fly heads (*daGal4* > KK control vs *daGal4* > *dTrmt10A* RNAi). **(B)** IGV genome browser tracks of m⁶A-IP and Input reads for *Hsp70* genes in basal conditions, from control and *dTrmt10A* RNAi. Red box highlights increase of 5'UTR m⁶A with *dTrmt10A* RNAi. **(C)** RT-qPCR shows decreased levels of *Hsp70* RNA in basal conditions from KK control and *dTrmt10A* RNAi brains. t-test, ***p* < 0.01. **(D)** *dTrmt10A* RNAi decreased protein levels of *Hsp70* in basal and HS conditions. t-test, **p* < 0.05. **(E)** *daGal4* > KK control vs *daGal4* > *dTrmt10A* RNAi and *elavGal4* > KK control vs *elavGal4* > *dTrmt10A* RNAi increased heat stress sensitivity of the animals. Animals heat stressed for 1 h at 38.5 °C and allowed to recover for 24 h. t-test, ****p* < 0.001. ***p* < 0.01. **(F)** Scatterplot of normalized read coverage of m⁶A-IP/input for 5'UTR of m⁶A transcripts in control versus *dTrmt10A* RNAi conditions. *dTrmt10A* RNAi shows a shift towards increased m⁶A levels in 5'UTR. **(G)** Genome browser tracks of m⁶A-IP and Input reads for *DnaJ-1* in basal conditions, from control and *dTrmt10A* RNAi. Red box highlights increased 5'UTR m⁶A upon *dTrmt10A* upregulation. RADAR differential peak analysis in Supplemental Data 2. **(H)** RNA decay assay from Control and *dTrmt10A* RNAi fly brains, dissected and incubated in Schneider's *Drosophila* Medium plus 169.5 μg/ml of actinomycin D for 4 h. RNA was extracted and used for RT-qPCR to determine relative RNA levels of *Rpl32*, and *Hsp70*. Data are presented as mean ± SD of *n* = 4 biological replicates, 12 brains per replicate. ***p* < 0.01. Student's two-tailed t-test. ns = not significant.

chaperones revealed 5'UTR m⁶A normally present at baseline on *Hsp70* transcripts was lost upon *dTrmt10A* upregulation, conferring the opposite effect from *dTrmt10A* RNAi (Fig. 3B). Additionally, Hsp70 RNA and protein levels were elevated in UAS-*dTrmt10A* brains (Fig. 3C,D), and animals were more resilient to heat stress (Fig. 3E). Loss of *Mettl3* also leads to elevated Hsp70 transcript and protein levels. To provide support that the change in Hsp70 with *dTrmt10A* upregulation was due to effects on m⁶A, vs other possibilities, we simultaneously reduced *Mettl3* and upregulated *dTrmt10A* in neurons. Co-expression of *Mettl3* RNAi and UAS-*dTrmt10A* in the brain showed a similar increase in Hsp70 protein levels compared to expression of either transgene alone (Fig. 3F). These data suggest that *dTrmt10A* is acting through the m⁶A/*Mettl3* pathway to modulate Hsp70 levels.

Similar to *Mettl3* RNAi brains, *dTrmt10A* upregulation significantly reduced 5'UTR m⁶A on *DnaJ-1* (Hsp40 chaperone), and UAS-*dTrmt10A* brains had increased protein levels of *DnaJ-1* (Fig. 3G,H). RNA decay analysis indicated upregulation of *dTrmt10A* led to higher stability of *DnaJ-1* RNA while there was no significant difference observed in the RNA levels of the unmodified *RpL32* transcript (Fig. 3I). Overall, *dTrmt10A* upregulation showed similar effects on heat shock chaperone levels and heat shock resilience as observed with *Mettl3* RNAi⁴⁶. Elevated levels of stress chaperones at baseline in the brain potentially precondition the brain to acute heat stress. Taken together, these data highlight that upregulation of *dTrmt10A* reduces m⁶A levels and confers heat stress resilience.

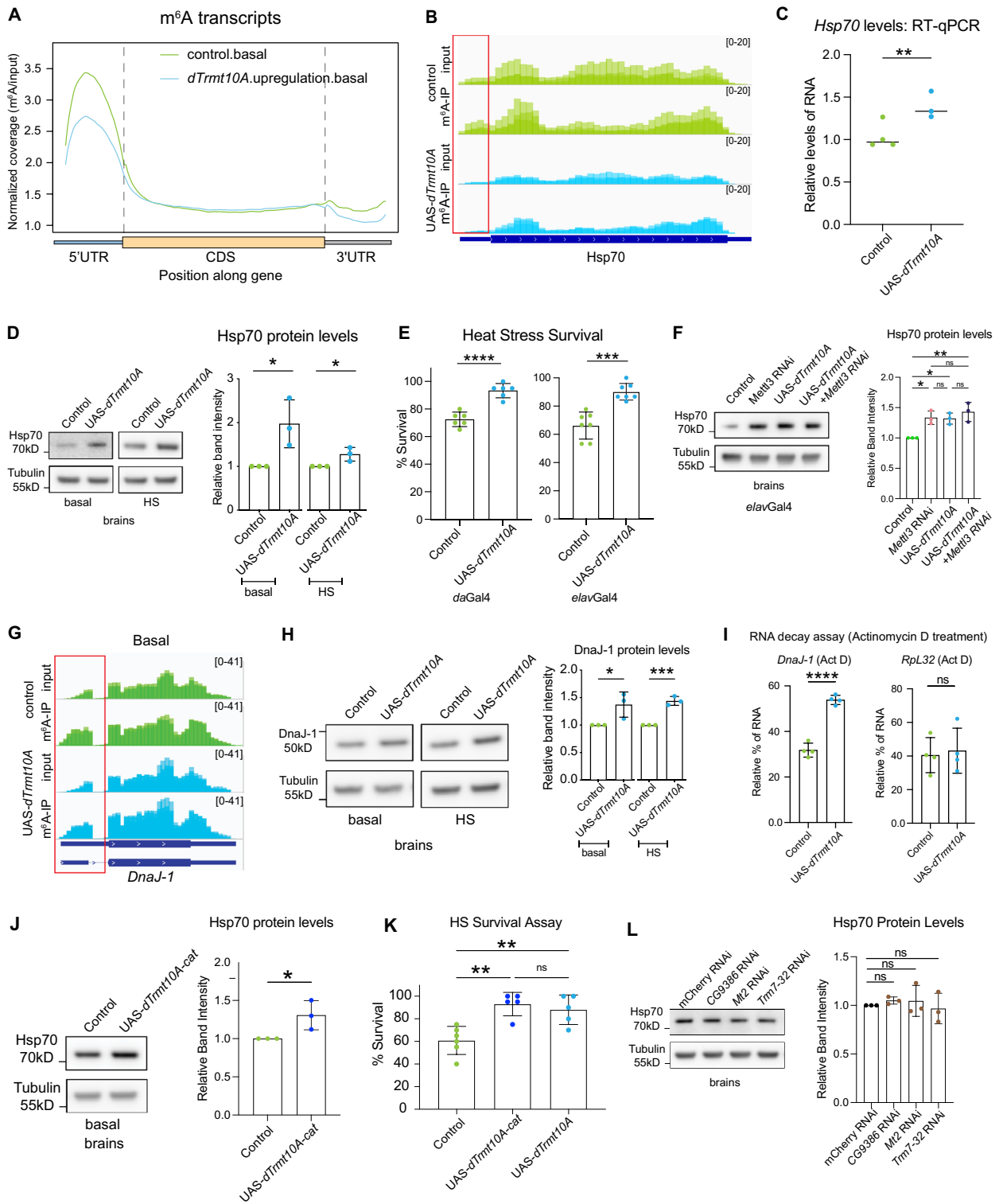
Because *dTrmt10A* is a tRNA methyltransferase, we performed additional experiments to confirm that its role to modulate Hsp70 and the stress response is due to an impact on m⁶A, and not its role as a tRNA methyltransferase. We generated animals that expressed *dTrmt10A* with a known mutation in the conserved m¹G catalytic domain of the methyltransferase activity that abolishes tRNA methyltransferase activity in vitro¹⁴ (G206R; see Fig. 1A). We assessed the impact of this mutation using sensitive readouts of *dTrmt10A* function: the levels of Hsp70 and animal stress sensitivity. Baseline levels of Hsp70 were increased in the brains of the animals expressing the catalytic mutant (UAS-*dTrmt10a-cat*), and these animals had increased stress resilience comparable to wild type (Fig. 3J,K). These data indicate that the phenotypic effects of *dTrmt10A* on Hsp70 and stress resilience are not dependent on the m¹G catalytic activity. We also examined three additional tRNA methyltransferases for effects on Hsp70 levels. RNAi of these additional tRNA methyltransferases (*CG9386* RNAi, *Mt2* RNAi, *Trm7-32* RNAi) had no effect on basal Hsp70 levels in the brain (Fig. 3L). Together these data indicate that the effects of *dTrmt10A* on Hsp70 levels and stress resilience are independent of its catalytic activity as a tRNA methyltransferase, and are not a general property of compromised tRNA methyltransferase activity.

Upregulation of *dTrmt10A* mimics loss of methyltransferase *Mettl3*, and globally decreases m⁶A on neurogenesis and signaling transcripts.

A total of 675 transcripts showed differential m⁶A methylation upon *dTrmt10A* upregulation, and only a few of these transcripts were HS chaperones (Fig. 4A). To investigate *dTrmt10A* further, we compared the m⁶A sites from *dTrmt10A* upregulation m⁶A-IP to the defined *Mettl3*-dependent methyltransferase m⁶A sites and transcripts⁴⁶. 62% of the transcripts from genes with *Mettl3*-dependent m⁶A were also regulated by *dTrmt10A* (Fig. 4A). We focused on these transcripts, as m⁶A is *Mettl3*-dependent. Closer analysis of these methylated transcripts revealed 41% of *dTrmt10A*-dependent m⁶A sites were in the 5'UTR, while 48% were in the 3'UTR (Fig. 4B), with a small number (81 genes) showing both 5'UTR and 3'UTR-dependent m⁶A changes (Fig. 4C). Modulation of m⁶A on the 3'UTR of transcripts was surprising due to the enrichment of m⁶A on the 5'UTR in *Drosophila*^{3,46–48}. This finding suggests that *dTrmt10A* may have a specialized role to regulate 3'UTR m⁶A. When we examined all *Mettl3*-dependent m⁶A transcripts with peaks in either the 5'UTR (Fig. 4D) or 3'UTR (Fig. 4E) regions; there was a similar shift towards decreased m⁶A-IP/Input enrichment upon *dTrmt10A* upregulation for both regions of transcripts. Reactome and KEGG^{49,50} pathway analyses showed that these transcripts are enriched for dynamic signaling pathways and axon guidance pathways (Fig. 4F and Supplementary Data 3). Similar GO terms were enriched regardless of 5'UTR or 3'UTR modification site.

We examined select targets with available antibodies (*Nrg*, *Myc*, and *fl(2)d*) to determine whether *dTrmt10A*-dependent m⁶A modification of transcripts impacted protein levels. Upregulation of *dTrmt10A* showed decreased m⁶A on these transcripts, and we observed increased protein levels in *Drosophila* brain tissue (Fig. 4G,H). These findings support previous work in mammalian cells that observe changes in *Myc* levels due to m⁶A-TRMT10A interaction²⁷. We extended these data to global protein synthesis using a puromycin assay to assess nascent protein synthesis. These data showed that upregulation of *dTrmt10A* was associated with increased puromycin incorporation, thus increased global nascent protein translation in the brain (Supplementary Fig. 1D). We observed the opposite response in puromycin levels upon *dTrmt10A* RNAi (Supplementary Fig. 1D). The catalytic mutant animals still showed increased global protein synthesis in the brain by puromycin assay (Supplementary Fig. 1E), confirming that puromycin changes are not due to m¹G activity of *dTrmt10A*. The additional tRNA methyltransferases, which did not impact Hsp70 protein levels, also did not affect global puromycin incorporation (Supplementary Fig. 1F). Therefore, *dTrmt10A* modulation of m⁶A transcripts likely leads to the influence on overall protein levels in the brain.

Many chromatin regulatory RNAs are m⁶A modified, and m⁶A methyltransferase complex components are known to bind chromatin and regulate transcription elements and histone modifications^{51,52}. We therefore considered whether *dTrmt10A* may also be associated with chromatin. *dTrmt10A* was overexpressed in the *Drosophila* salivary glands and *dTrmt10A* protein localization was examined on the large polytene chromosomes by immunostaining to the HA tag. *dTrmt10A* showed robust localization to the nucleolus as anticipated for its role in tRNA modification; however, *dTrmt10A* also showed binding to band locations on the polytene chromosomes (Supplementary Fig. 2A). Chromatin immunoprecipitation followed by western immunoblot validated *dTrmt10A* association with chromatin (Supplementary Fig. 2B) and chromatin binding was not dependent



◀Figure 3. *dTrmt10A* upregulation confers heat stress resilience. **(A)** Normalized read coverage plot of m⁶A-IP/ input on polyA + transcripts in the 5'UTR, CDS, and 3'UTR of m⁶A modified transcripts. m⁶A-IP sequencing in basal conditions from control fly (*daGal4* > KK control) versus *dTrmt10A* upregulation (*daGal4* > UAS-*dTrmt10A*) heads. **(B)** IGV genome browser tracks of m⁶A-IP enrichment versus Input reads for Hsp70 in basal conditions, from control (*daGal4* > KK control) and *dTrmt10A* upregulation (*daGal4* > UAS-*dTrmt10A*). Red box highlights loss of 5'UTR m⁶A with *dTrmt10A* upregulation. **(C)** RT-qPCR of Hsp70 RNA levels in basal conditions from control (*daGal4* > KK control) and *dTrmt10A* upregulation (*daGal4* > UAS-*dTrmt10A*) brains. t-test, ***p* < 0.01. **(D)** Upregulation of *dTrmt10A* increased protein levels of Hsp70 in basal and heat stress conditions. *daGal4* > KK control vs *daGal4* > UAS-*dTrmt10A*, *elavGal4* > KK control vs *elavGal4* > UAS-*dTrmt10A* t-test, **p* < 0.05. **(E)** Upregulation of *dTrmt10A* (*daGal4* > Control vs. UAS-*dTrmt10A* or *elavGal4* > Control vs UAS-*dTrmt10A*) increased animal heat stress survival. t-test, *****p* < 0.0001, ****p* < 0.001. **(F)** Hsp70 protein levels from brains. *elavGal4*;mCherry RNAi > UAS-mcd8GFP vs *elavGal4*;Mettl3 RNAi > UAS-mcd8-GFP vs *elavGal4*;mCherry RNAi > UAS-*dTrmt10A* vs *ElavGal4*;Mettl3 RNAi > UAS-*dTrmt10A*, n = 3 biological replicates, **p* < 0.05, ***p* < 0.01 One-way ANOVA. **(G)** Genome browser tracks of m⁶A-IP and Input reads for *DnaJ-1* in basal conditions, from control and UAS-*dTrmt10A*. Red box highlights loss of 5'UTR m⁶A with *dTrmt10A* upregulation. **(H)** Upregulation of *dTrmt10A* increased protein levels of DnaJ-1 in basal and HS conditions. t-test, **p* < 0.05, ****p* < 0.001. RADAR differential peak analysis in Supplemental Data 2. **(I)** RNA decay assay from Control, and UAS-*dTrmt10A*, in the presence of actinomycin D, to determine relative RNA levels of *RpL32* and *DnaJ-1*. Data are presented as mean ± SD of n = 4 biological replicates, 12 brains per replicate. *****p* < 0.0001. Student's two-tailed t-test. ns = not significant. **(J)** UAS-*dTrmt10A-cat* increased protein levels of Hsp70 in basal brain conditions. *daGal4* > KK control vs *daGal4* > UAS-*dTrmt10A-cat*, t-test, **p* < 0.05. **(K)** *daGal4* > UAS-*dTrmt10A-cat* mutant increased heat stress resilience of the animals. Animals heat stressed for 1 h at 38.5 °C and allowed to recover for 24 h. One-way ANOVA, ***p* < 0.01. **(L)** Hsp70 protein levels in basal brains with knockdown of additional tRNA methyltransferases. *daGal4* > mCherry RNAi, *daGal4* > CG9386 RNAi, *daGal4* > Mt2 RNAi, *daGal4* > Trm7-32 RNAi, One-way ANOVA, ns = not significant.

on RNA (Supplementary Fig. 2C). These data indicate that *dTrmt10A* is positioned for an additional layer to m⁶A-modified gene regulation on chromatin, similar to *Mettl3*^{51,53}.

With stress, *dTrmt10A* primarily impacts 3'UTR m⁶A sites

Based on the heat stress resilience of upregulated *dTrmt10A*, we looked more closely at the regulation of m⁶A during heat stress with overexpression of *dTrmt10A*. We performed acute heat shock (HS) experiments then analyzed m⁶A-IP from *Drosophila* head polyA + RNA. These data showed that *dTrmt10A* upregulation reduced overall m⁶A levels in both basal and HS conditions (Fig. 5A). Interestingly, *dTrmt10A* upregulation led to modification of mostly 3'UTR m⁶A sites during heat stress, with 73% of *dTrmt10A*-dependent sites located in this region of transcripts upon HS (Fig. 5B).

Upon heat stress and *dTrmt10A* upregulation, there was a shift towards increased expression of m⁶A marked transcripts (Fig. 5C, blue vs black). Furthermore, the majority of these differentially expressed transcripts exhibited *dTrmt10A*-dependent m⁶A modifications on their 3' UTR (Fig. 5D). Notably, there was no trend in the levels of non-m⁶A modified transcripts, with equal numbers of transcripts being up and downregulated between control and *dTrmt10A* upregulation (Fig. 5C). Among the m⁶A transcripts, we identified critical genes involved in signaling processes and neurogenesis, such as *pAbp*, *SK*, *para*, *Sh*, *bru3* and even the nuclear m⁶A reader protein *Ythdc1* (Fig. 5E and Supplementary Fig. 3A). These findings highlight the essential role of *dTrmt10A* in m⁶A modification during stress, particularly in modifying transcripts that are integral to neuronal signaling processes.

Compared to other tissues, many genes in the *Drosophila* nervous system have substantially extended 3'UTRs and alternative polyadenylation^{54,55}. We found that 25% of *Drosophila* CNS transcripts with extended 3'UTRs also have m⁶A modification in their 3'UTR (Supplementary Fig. 3B). Furthermore, this subset of m⁶A transcripts are enriched for cognition, learning, and memory pathways, indicating this subclass of 3'UTR m⁶A modified transcripts are alternatively polyadenylated and involved in learning and memory. We also examined the overall length of 3'UTRs of m⁶A modified transcripts and found that the average length of their 3'UTR was longer compared to all 3'UTR weighted lengths from wildtype *Drosophila* CNS⁵⁵ (Supplementary Fig. 3C).

Proteins that interact with *dTrmt10A*

In mammalian cells, TRMT10A regulates m⁶A by interacting with the m⁶A demethylase FTO. Although there are no known homologs in *Drosophila* to the demethylases FTO or ALKBH5, we considered that a fly demethylase, should it exist^{24,27,56}, may interact with *dTrmt10A*. To define interacting proteins, we expressed UAS-*dTrmt10A-HA* and immunoprecipitated *dTrmt10A* from *Drosophila* head lysates using the HA tag. Mass spectrometry was used to evaluate enriched protein interactions of *dTrmt10A-HA* compared to IgG control (Supplementary Data 4). This analysis identified 6 high confidence interacting proteins (Pp1-87B, CG18680, CG9953, hrm, Dhx15), with no apparent homologs to FTO or ALKBH5. When we analyzed all interactions (low, medium, and high), there was enrichment for proteins involved in RNA metabolism and deadenylation, including DCP1, Atx2, twin, and Rga, as well as proteins involved in translation regulation, such as eIF3a (Fig. 6A). These proteins may interact with and regulate downstream m⁶A-modified RNA processing through interaction with *dTrmt10A*. We also investigated whether *dTrmt10A* binds or alters the levels of known m⁶A regulators such as *Mettl3* or m⁶A reader proteins *Ythdc1* or *Fmr1*, but found no interaction or altered protein levels (Supplementary Fig. 4), indicating that *dTrmt10A* does not interact with these known m⁶A binding proteins to mediate its effect on m⁶A.

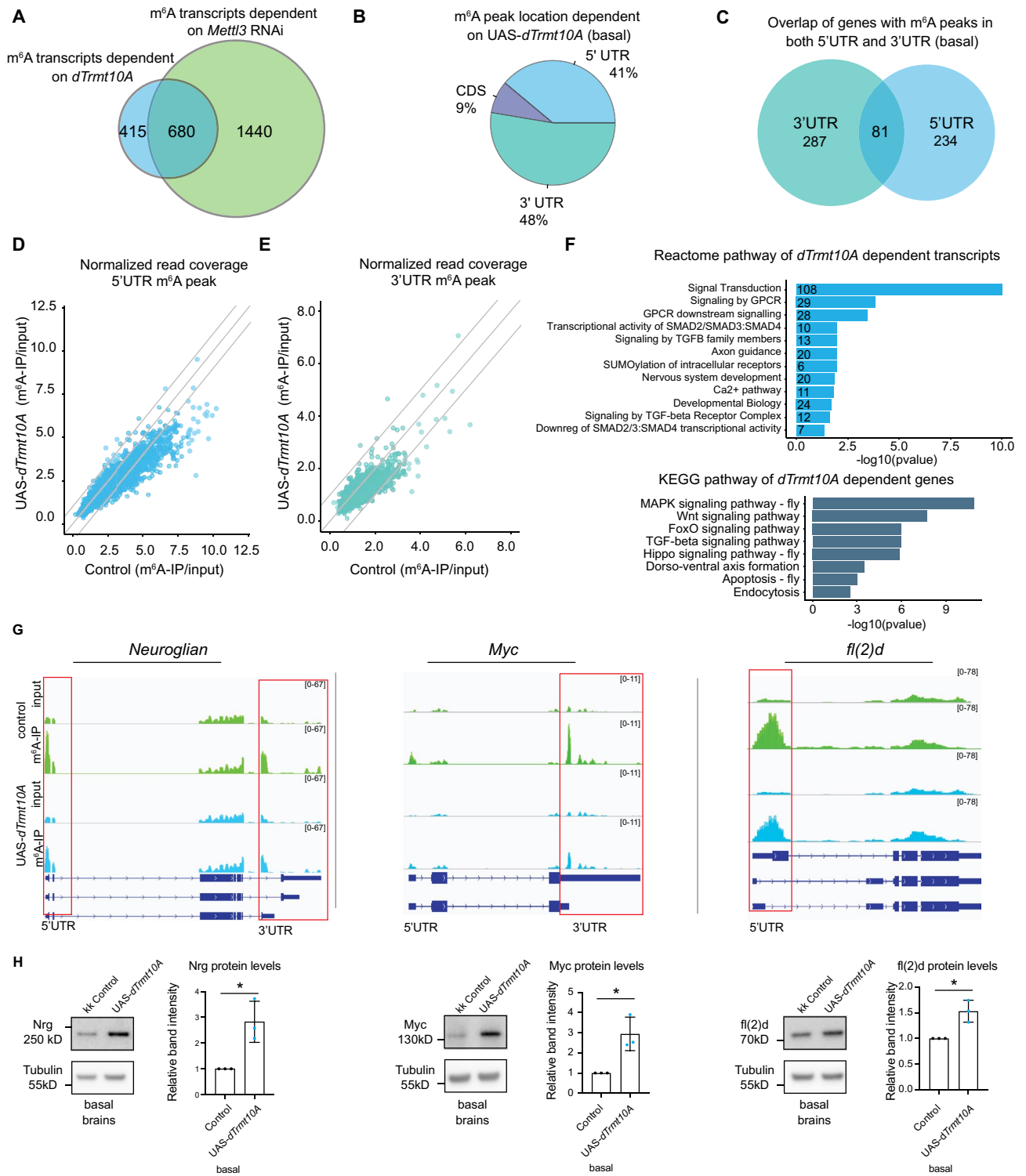


Figure 4. *dTrmt10A* upregulation decreases m⁶A on neurogenesis and signaling pathway transcripts. (A) Overlap of *dTrmt10A*-dependent m⁶A from the m⁶A-IP sequencing experiment, and *Mettl3*-dependent m⁶A transcripts (from⁴⁶). We focused on the 680 transcripts that are overlapping as *dTrmt10A*-dependent targets. (B) Percent location of *dTrmt10A*-dependent m⁶A at baseline indicates an enrichment for 3'UTR m⁶A regulation. (C) Overlap of *dTrmt10A* m⁶A targets with 5'UTR peaks and those with 3'UTR peaks; some transcripts have m⁶A in both locations. List of genes given in Supplemental Data 2. (D–E) Scatterplot of normalized read coverage of m⁶A-IP/input for 5'UTR (left) or 3'UTR (right) of m⁶A transcripts in control versus UAS-*dTrmt10A* conditions. *dTrmt10A* upregulation shows a shift towards decreased m⁶A levels. (F) Pathway analysis and Kegg term^{49,50} analysis of all *dTrmt10A*-dependent m⁶A transcripts shows enrichment for signaling and neuronal pathways. (G) IGV genome browser tracks of m⁶A-IP enrichment versus Input reads for *Nrg*, *Myc*, and *fl(2)d* in basal conditions, from control and UAS-*dTrmt10A*. Red box highlights loss of 5'UTR or 3'UTR m⁶A with *dTrmt10A* upregulation. (H) *Nrg*, *Myc*, *fl(2)d* protein levels from control or UAS-*dTrmt10A* brains dissected in basal conditions. Quantification of 3-biological replicate immunoblots, 15 brains per replicate, showing increased expression of protein in (*daGal4*>UAS-*dTrmt10A*) fly brain. Data are presented as mean ± SD, t-test **p*<0.05.

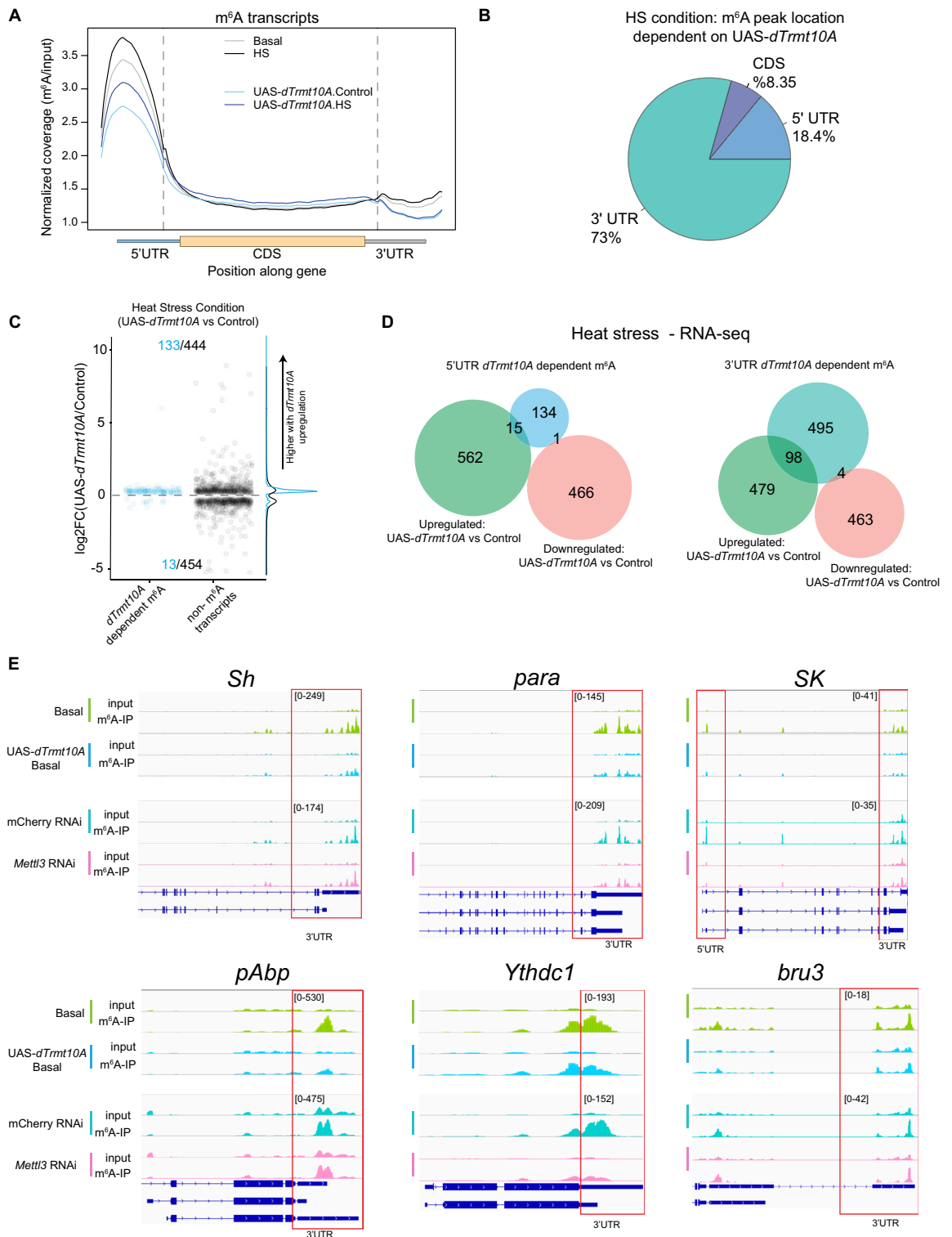


Figure 5. *dTrmt10A* upregulation shows more 3'UTR m⁶A peak changes with heat stress (HS). (A) Normalized read coverage plot of m⁶A-IP/input on polyA+ transcripts in the 5'UTR, CDS, and 3'UTR of m⁶A modified transcripts. m⁶A-IP sequencing in basal and HS conditions from control (*daGal4* > KK control) versus *dTrmt10A* upregulation (*daGal4* > UAS-*dTrmt10A*) heads. (B) Location of *dTrmt10A* dependent m⁶A indicates enrichment for 3'UTR m⁶A regulation upon HS. (C) Plot of significantly differentially expressed genes in *daGal4* > KK control vs > UAS-*dTrmt10A* heads in HS condition. Positive logFC indicates an increase in transcript levels in *dTrmt10A* upregulation heads. m⁶A genes (blue), or all other genes (black). (D) Venn diagram of 5'UTR or 3'UTR *dTrmt10A* m⁶A marked transcripts with genes that are differentially expressed in control vs UAS-*dTrmt10A* in HS conditions. (E) IGV genome browser tracks of m⁶A-IP enrichment versus Input reads for transcripts in basal conditions, from KK control and UAS-*dTrmt10A*. Bottom four lanes depict IGV tracks from mCherry RNAi control and *Mettl3* RNAi in basal conditions. These peaks show dependence on *Mettl3* and UAS-*dTrmt10A* by RADAR analysis. Red box highlights 3'UTR m⁶A. Values denote data range on IGV browser for either UAS-*dTrmt10A* or *Mettl3*.RNAi sequencing experiments.

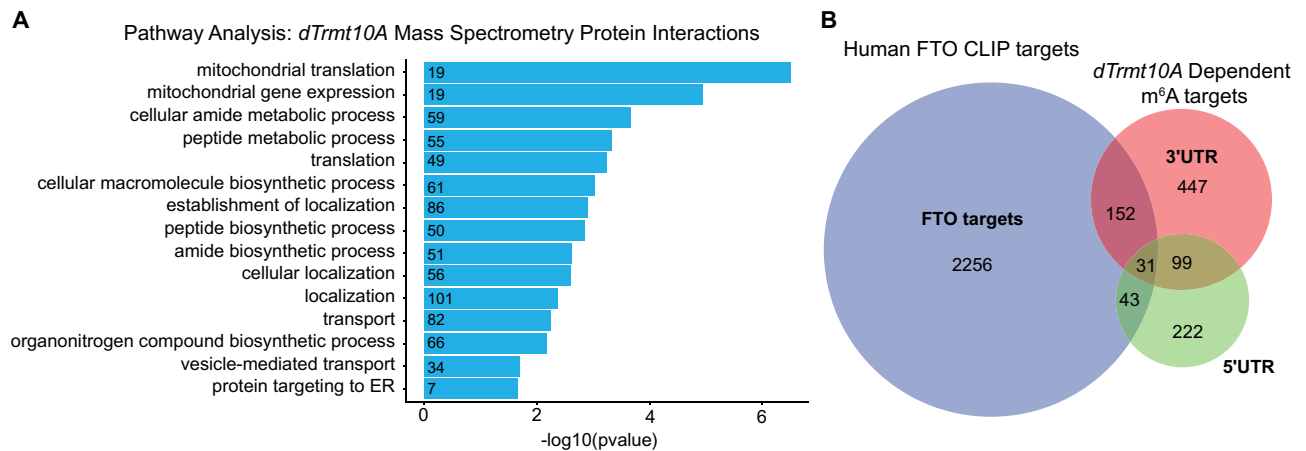


Figure 6. *dTrmt10A* co-IP interactions from head lysates. **(A)** Affinity purification of HA-tagged *dTrmt10A* followed by protein mass spectrometry to identify *dTrmt10A*-associated proteins. GO term analysis of proteins shown to have a positive interaction with *dTrmt10A*. Genes above 1.3 LogFC selected as positive interaction. $-\log_{10}(\text{pvalue})$ enrichment of genes and number of genes in each category is shown. See Supplementary Data 4 for full protein list and GO terms with *p*-values. **(B)** Human FTO CLIP targets (Ontiveros, R Jordan et al. 2020²⁷), overlapped with m⁶A gene targets modified in the 5'UTR or 3'UTR m⁶A by upregulation of *dTrmt10A*. Mass spectrometry proteins and GO analysis genes listed in Supplemental Data 4.

Both mammalian and *Drosophila* m⁶A-modified transcripts are enriched for similar biological pathways^{22,30,57}, highlighting the importance of m⁶A in signaling and stress. Although a candidate demethylase is not identified in *Drosophila*, we used FTO CLIP targets from mammalian cells²⁷ to define the homologous *Drosophila* genes. We compared these FTO CLIP targets to *dTrmt10A*-dependent m⁶A transcripts and found that ~23% of *dTrmt10A*-dependent m⁶A transcripts overlap with FTO targets (Fig. 6B). This overlap is similar to the extent of overlap of transcript targets between TRMT10A and FTO in mammalian cells (35%²⁷). Notably, 3'UTR m⁶A transcripts showed a greater overlap with FTO targets (Fig. 6B). These data suggest that the interaction of *dTrmt10A* toward 3'UTR m⁶A RNA binding proteins and/or a putative demethylase may fine-tune aspects of RNA processing.

Discussion

This study offers valuable insights into the *in vivo* role of *dTrmt10A* on m⁶A modification within the *Drosophila* brain, and its impact on stress resilience and gene regulation. Of note, *dTrmt10A* modulates m⁶A peaks both on the 5'UTR of transcripts (where most m⁶A peaks are in *Drosophila* transcripts), but also on the 3'UTR of *Drosophila* genes. Upregulation of *dTrmt10A* caused a global decrease in m⁶A levels on transcripts and increased the animal's resilience to heat stress, with increases in overall protein and RNA levels of key players like Hsp70 (see Figs. 3 and 4). These findings highlight that *Drosophila* transcripts are modulated by m⁶A in the 3'UTR in addition to 5'UTR, confirming that m⁶A modification plays a crucial role in dampening the biological response of the brain to acute stress, and that *dTrmt10A* acts as an additional regulator of m⁶A modification of transcripts in the brain. Moreover, modulation of *dTrmt10A* showed the ability to modulate m⁶A peak levels in transcripts, despite not being a canonical component of the methyltransferase complex (Fig. 7). *dTrmt10A* with a mutation in the m¹G catalytic domain of the tRNA methyltransferase functioned similarly in our assays as the wild-type protein, and additional *Drosophila* tRNA methyltransferases failed to show these phenotypes, confirming that the function of *dTrmt10A* as a tRNA methyltransferase is not influencing Hsp70 protein levels and protein translation. There are many known mutations in human TRMT10A that impact brain development^{13–15}, and these data now indicate that the function of TRMT10A/*dTrmt10A* on m⁶A levels may also play a role in these diseases.

m⁶A modification in brain homeostasis

Many biological functions in the brain are regulated by RNA modification, including axon growth, embryonic stem cell fate, learning and memory, and neurogenesis^{30,58}. Furthermore, mutations in RNA modification proteins have been linked to compromised cellular stress responses, tumorigenesis, and severe developmental defects^{9,10,20,33,38}. Our findings contribute to the current knowledge of RNA modifications regulating the neuronal response to cellular stress, and the regulation of m⁶A overall in the brain. *dTrmt10A* regulated m⁶A levels on signaling pathway transcripts, such as MAPK and WNT signaling pathways that are critical for normal neuronal homeostasis. These signaling pathway transcripts were also regulated by *Mettl3*, the m⁶A methyltransferase. We validated m⁶A changes using *Mettl3* knockdown and cross compared to other *Drosophila* studies; future non-antibody detection techniques would be important to apply.

Although m⁶A methylation primarily occurs in the 5'UTR of transcripts in *Drosophila*, *dTrmt10A* upregulation surprisingly skewed towards selective 3'UTR m⁶A regulation. Thus far, little is understood regarding why m⁶A is highly enriched in the 5'UTR of *Drosophila* transcripts vs 3'UTR as in mammals; however, *dTrmt10A* has uncovered that m⁶A regulation occurs in the 3'UTR of transcripts in *Drosophila*. Many critical signaling and neurogenesis transcripts such as *Sh*, *bru3*, *para*, and *pAbp* contain *dTrmt10A*-dependent m⁶A in the 3'UTR. Additionally, these transcripts were upregulated in brains with increased *dTrmt10A* expression, indicating they

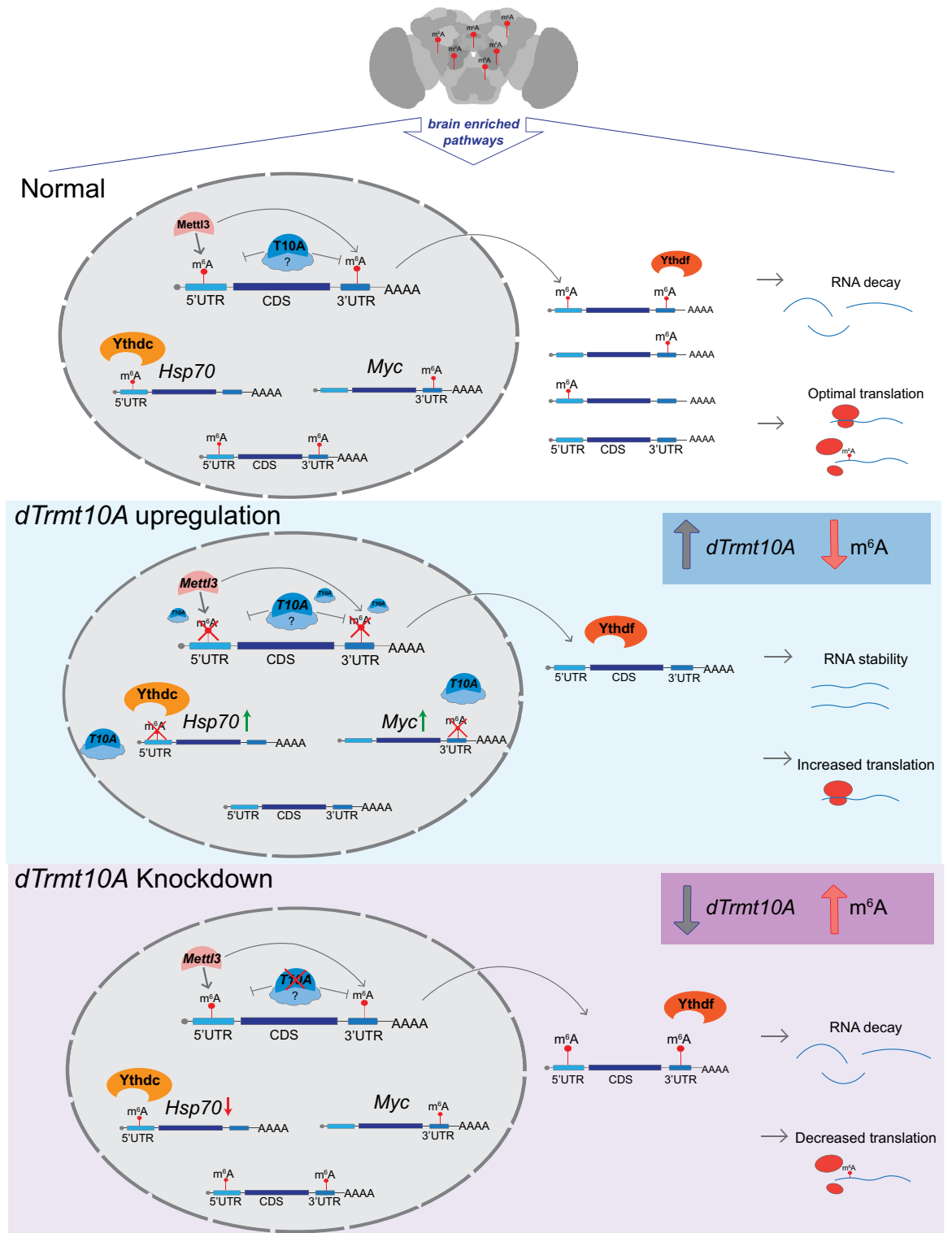


Figure 7. Model of *dTrmt10A* regulation in the brain. m⁶A is highly enriched in the *Drosophila* brain, and marks transcripts enriched in dynamic signaling and neuronal growth pathways. *dTrmt10A* upregulation reduces m⁶A levels in the 5'UTR and 3'UTR of transcripts. *Myc* and *Hsp70* are example genes that show increased protein levels with *dTrmt10A* upregulation. *dTrmt10A* upregulation leads to increased RNA and protein levels of these transcripts. Conversely, *dTrmt10A* knockdown shows a dramatic increase in 5'UTR m⁶A, with significance for *Hsp70*. *dTrmt10A* upregulation modulates heat stress chaperones of *Drosophila* such that animals are more stress resilient.

become more stabilized by loss of m⁶A modification. Transcripts of *Myc* and *Nrg* with 3'UTR m⁶A showed increased protein levels with *dTrmt10A* upregulation. These findings suggest that both 3'UTR and 5'UTR m⁶A serve functionally to keep transcript and protein levels low in the *Drosophila* brain. Furthermore, m⁶A marked transcripts are enriched in neural and dynamic signaling processes, indicating that one mechanism by which the brain regulates precise dynamics of neural signaling pathways may be through marking key transcripts with m⁶A for tighter control. Dysfunction in m⁶A is therefore predicted to have a larger impact on those transcripts critical for neural function. Additionally, we find that many 3'UTR m⁶A transcripts also have extended 3'UTR lengths in the *Drosophila* nervous system. A detailed analysis of *dTrmt10A* effect on alternative polyadenylation may be of interest, particularly within the context of the *Drosophila* nervous system, given the enrichment of the transcripts in learning, memory, and cognition.

We speculated that *dTrmt10A* may interact with a demethylase, similar to the mammalian enzyme. By mass spectrometry analysis of dTrmt10A IPed from head lysates and defining the interacting proteins, an obvious candidate was not revealed. The absence of a demethylase homologous to FTO in the fly suggests alternative mechanisms may be at play, such as interactions with RNA-binding proteins involved in decay. Additionally, dTrmt10A could impact proteins within the methyltransferase complex, which themselves have a more direct role on m⁶A modification; for example, dTrmt10A modulated fl(2)d levels. The mass spectrometry analysis showed dTrmt10A associates with key RNA degradation components including DCP1, Twin, and Rga. Thus, through interaction with dTrmt10A, these proteins may confer specificity and degradation impact of dTrmt10A on m⁶A targets. Furthermore, disease-associated protein Atx2, mutated in spinocerebellar ataxia 2, was found to co-IP with dTrmt10A. Atx2 is involved in RNA metabolism including RNA stability, RNA localization to stress granules and P-bodies, and interacts with other disease-associated RNA binding proteins such as TDP-43⁵⁹. We also compared *dTrmt10A*-m⁶A modified transcripts to human FTO CLIP RNA targets. There was a significant overlap, and the degree of overlap was comparable to that of mammalian cells²⁷. The overlapped targets are enriched for signaling pathways, similar to GO term analysis of all m⁶A targets⁴⁶. Considering that *Drosophila* m⁶A is predominantly deposited in the 5'UTR, we were surprised to find more m⁶A transcripts modified in the 3'UTR that overlapped with FTO targets, indicating specificity in potential demethylase/degradation targeting.

Cellular stress and m⁶A modifications

To reduce cellular burden during stress, global protein synthesis is repressed and non-essential RNAs are decayed or stored in stalled mRNA-protein granules. During this process, vital RNAs are translated for stress survival. In the recovery phase, stress mediated RNAs are in turn decayed and RNAs necessary for normal cell maintenance are once again transcribed and translated³⁶. The process of stress response activation and resolution is a fine-tuned dance of RNA decay and translation, such that prolonged stress or failure to activate stress machinery is detrimental. RNA modifications have emerged as critical regulators of dynamic signaling in normal cell maintenance and also during stress recovery^{20,31,38}. Particularly neurons, which are postmitotic and cannot remove harmful accumulations through cell division, show specialized mechanisms to combat cellular stress.

In mammalian cells m⁶A modification has been shown to increase upon heat stress in the 5'UTR of *Hsp70* to facilitate cap-independent translation²⁶. Other studies in vitro indicate that *Hsp70* becomes co-transcriptionally marked by m⁶A, which leads to its degradation³⁹. Furthermore during stress resolution, the lncRNA *Heat*, a transcriptional activator of HSF1, becomes heavily methylated by m⁶A, and Ythdc1 degrades the lncRNA to prevent stress gene activation⁴⁰. In the *Drosophila* brain, *Hsp70* is m⁶A modified in the 5'UTR at baseline, and m⁶A is lost upon acute heat stress⁴⁶. We hypothesize this limits *Hsp70* translation at baseline and that the loss of m⁶A facilitates accumulation of the transcript for translation during stress. Thus, loss of m⁶A in the 5'UTR of *Hsp70* leads to elevated levels of *Hsp70* protein, which may allow for a state of preconditioning of the brain to future stress. With *dTrmt10A* knockdown, we were surprised to see a dramatic increase in 5'UTR m⁶A on *Hsp70*—especially given that no other transcripts showed such a dramatic increase in m⁶A. These data indicate that stress resilience may be a particularly important target of *TRMT10A/dTrmt10A* gene mutation.

In summary, using m⁶A-IP sequencing, we find that *dTrmt10A* impacts 5'UTR m⁶A methylation on key stress chaperones, but *dTrmt10A* also highlights that 3'UTR m⁶A occurs and is regulated in *Drosophila*. These studies provide a framework for future insight into how m⁶A regulation is achieved at specific sites, like the 5'UTR vs 3'UTR. These data reveal that additional m⁶A regulators like *dTrmt10A* outside of the core complex components may profoundly modulate region specific methylation and/or demethylation. m⁶A regulation in the brain likely serves to fine tune signaling pathways for the continued maintenance of axons and dynamic synaptic connections. This comes at the cost of dampening the acute stress response, which compromises the overall ability of the brain to withstand insults. Given that mutations in *TRMT10A* are associated with developmental brain disease, some mutations that compromise *TRMT10A* function may also include impacts on m⁶A and stress resistance.

Materials and methods

Drosophila stocks and maintenance

A full list of *Drosophila* stocks used in this study are described in Supplementary Data 1. RNAi and UAS lines were generated by the Harvard Transgenic RNAi Project (TRiP) and the Vienna *Drosophila* Resource Center (VRDC)^{60,61}, and stocks were obtained from the Bloomington *Drosophila* Stock Center, Indiana, USA. Crosses were performed at 25 °C and grown on standard cornmeal molasses agar. Driver lines used: *daGAL4*, *elavGal4*, *nSybGal4* as indicated per experiment. For all experiments male flies were used, for consistency in the experiments, and to avoid issues in food consistency due to egg laying of females.

Brain dissections

Brain dissections were conducted as previously described⁶². Briefly, flies were anesthetized using CO₂ and decapitated using forceps. The head was placed posterior side down and the proboscis was then removed using Dumont #5 fine forceps (Fine Science Tools, 11254-20). The brain was then gently popped out through the proboscis cavity, cleaned in PBS, and transferred to an RNase free microfuge tube and PBS was aspirated. Brains were then ground in Laemmli Buffer (5 µL per brain, 10–20 brains for each sample) for Western immunoblotting, or in Trizol for RNA analysis.

Western immunoblot analysis

Brain or head samples were homogenized in sample buffer of 1 × Laemmli sample Buffer (Bio-rad, 1610737), 50 µl β-mercaptoethanol (Sigma, m6250), 1 × protease inhibitor (Roche, 11836170001), and 1 mM PMSF (Sigma, P7626). 50 µl of sample buffer is added per brain, 7.5 µl added per head, and 40 µl added per whole fly. Samples are boiled at 98 °C for 3 min, and then centrifuged at 1500 rpm for 3 min at room temp. Sample was loaded onto 15 well 1.0 mm 4%–12% Bis-Tris NuPAGE gels (Thermo Fisher, WG1401) with pre-stained protein ladder (Thermo Scientific, 22619). 1 brain, 1 head, or 8% of whole fly tissue is loaded on each lane per experiment. Gel electrophoresis was performed using Xcell Surelock Mini-Cell Electrophoresis System at 140 V, and transferred overnight onto a nitrocellulose membrane 0.45 µM (Bio-rad, 1,620,115), using a Bio-rad mini transblot cell at 90A for 16 h. Membranes were stained in Ponceau S (Sigma, P7170-1L), washed in DI water, and imaged with Amersham Imager 600. Ponceau S was washed off in 3 × 5 min in Tris-buffered saline with 0.1% Tween20 (TBST). Membrane was blocked in 5% non-fat dry milk (LabScientific, M08410) in TBST for 1 h, and incubated with primary antibodies with blocking buffer overnight at 4 °C. Following 3 × 5 min washed in TBST, membranes were incubated with HRP-conjugated secondary antibodies at 1:5,000 for 1 h at room temp in blocking solution. Membranes were washed 3 × 5 min in TBST and the signal was developed using ECL prime (Cytivia, #RPN2232) and detected using an Amersham Imager 600. Primary antibodies used: anti-tubulin (1:5000, DSHB, #AA4.3, Lot.5/31/18-44 µg/ml), anti-Hsp70 (1:5000, Sigma, #7FB-SAB5200204-100 µg, Lot.141002), anti-Mettl3 (1:5000, Proteintech, #15073-1-AP, Lot.Ag7110), anti-HSP40 (1:5000, Enzo Life Sciences, #ADI-SPA-400-D, Lot.04062141), anti-fl(2)d (1:10, #DSHB-9G2, Lot.10/18/18-42 µg/ml), anti-dFmr1 (1:500, #DSHB-5A11), anti-Nrg (1:600, #DSHB-BP104), anti-Myc (1:50, #DSHB-P4C4-B10), anti-puromycin (1:1000, Kerfast, #EQ0001, Lot.200517). Rabbit anti-Ythdc1 (1:5000) was created by Vivitide against 18 residues of Ythdc1 (157–173 “CRTKIPSNANDSAGHKSD”)⁴⁶. Secondary Antibodies used: Goat anti-mouse (1:5000, Jackson ImmunoResearch, #115-035-146, Lot.153978), Goat anti-Rabbit (1:5000, Jackson ImmunoResearch, #111-035-144, Lot.138306), Goat anti-rat (1:5000, Thermo Fisher Scientific, #A10549, Lot.2273679).

RNA extraction

Tissue was homogenized in 200 µl of Trizol (Thermo Scientific, #15596026) in RNase free 1.5 ml microfuge tubes (Thermo Scientific, #AM12400). 800 µl of Trizol (Thermo Scientific, #15596026) was added to the tube and 200 µl of chloroform (Fisher Scientific, #AC423555000) and was vigorously shaken for 20 s at room temp. Samples were left for 5 min at RT to form upper aqueous phase, and centrifuges at 4 °C for 15 min at 12,000 × g. The Upper aqueous phase was transferred to a fresh RNase free tube. RNA samples were then processed using the Zymo RNA clean & concentrator -5 kit (Zymo, #R1013), using their RNA clean-up from aqueous phase after Trizol /chloroform extraction protocol plus on column DNase I treatment. RNA amount was measured using a nanodrop and integrity was validated through on an Agilent 2100 Bioanalyzer using an RNA nano chip.

Real time PCR

400 ng RNA was used per cDNA reaction using the High Capacity cDNA Reverse Transcription Kit (Applied Biosystems, Thermo Scientific, #4368814). cDNA was then used for qPCR reactions set up with SYBR Green Fast Reagents, using a 384-well plates on the Applied Biosystems ViiA7 machine. Primers used are in Supplementary Data 1. Mean fold change was determined using the $\Delta\Delta C_t$ method. Each experiment used technical triplicates as well as three biological replicates, Graphpad prism 8/9 software was used for statistics.

Stress sensitivity assay

Fly crosses were carried out at 25 °C. Adult flies were collected and aged to 6d post eclosion. Flies were anesthetized and transferred to clear plastic 13 ml vials, and cotton was placed at the 4 ml mark on the vials to concentrate the flies near the bottom. Each vial contained 20 flies. Flies were allowed to recover for 30 min, and then transferred to a water bath for mild non-lethal heat stress (30 min at 38.5 °C) or a longer heat shock (1–1.5 h at 38.5 °C) for a severe stressor to measure stress sensitivity. The flies were then transferred to normal food and allowed to recover overnight at 25 °C. After recovery, the percent of flies alive versus dead was recorded per vial.

LC–MS/MS analysis of m⁶A levels

PolyA + RNA was extracted from brains, heads, and whole fly RNA using the NEBNext Poly(A) mRNA Magnetic Isolation Module (NEB, #E7490L). LC–MS/MS was conducted as previously described²⁷. All quantifications were performed by using the standard curve obtained from pure nucleoside standards running with the same group of samples. Then, the percentage ratio of m⁶A to A or m⁶G to G was used to compare the different modification levels.

m⁶A-IP sequencing

Total RNA was extracted from 200 *Drosophila* heads per replicate using Trizol/ chloroform extraction. PolyA + mRNA was obtained using NEBNext Poly(A) mRNA Magnetic Isolation Module. PolyA + RNA was fragmented using the NEBNext Magnesium Fragmentation Module (NEB, #E6150S) for 4 min at 95 °C for a 250 ng sample of polyA + RNA, and RNA was repurified using the Zymo RNA clean & concentrator -5 kit (Zymo, #R1013). 10% of the fragmented polyA + RNA was saved as an input control for sequencing. M⁶A -immunoprecipitation was done using the EpiMark N6-Methyladenosine Enrichment kit protocol with some minor alterations described. 30ul of protein G magnetic beads (NEB, #S1430) were washed and resuspended in IP buffer (150 mM NaCl, 10 mM Tris-HCL, 0.1% NP-40). 4ul of Synaptic Systems antibody (Synaptic Systems, #202003, Lot.2-119) was conjugated to protein G-magnetic beads (NEB, #E1611A, Lot.10015190) for 2 h at 4 °C. Beads/ antibody were washed twice in IP buffer. ~ 1 µg polyA + RNA was incubated with beads/antibody in IP buffer supplemented with 0.1% SUPERase-In RNase Inhibitor (Thermo Scientific; #AM2696) for 2 h at 4 °C. After incubation, RNA/beads/antibody are washed twice in IP buffer, twice in low salt IP buffer (50 mM NaCl, 10 mM Tris-HCL, 0.1% NP-40), and twice in high salt IP buffer (500 mM NaCl, 10 mM Tris-HCL, 0.1% NP-40). RNA is eluted from beads with 25 µl of RLT buffer twice and elution was pooled and concentrated using Zymo RNA clean and concentrator -5 kit (Zymo, #R1013). Libraries were made using SMARTer Stranded Total RNA-Seq Kit V2 without rRNA depletion (TakaraBio, #634411) for IPed and input RNA, and sequenced using illumina HiSeq X series with 40M paired end reads (2 × 150 bp). Library preparation and sequencing was done by Admera Health. Three biological replicates per genotype and condition were done with NEB m⁶A antibody, and two biological replicates were done with Synaptic Systems m⁶A antibody.

m⁶A enrichment analysis

Regions of m⁶A enrichment were found for each condition using MetPeak (v.1.1)⁶³ with default parameters, using the input and m⁶A pulldown bam files as input, and with the FlyBase FB2019_05 annotation provided. Peak locations (5' UTR, CDS, or 3' UTR) were defined from the regions indicated by MetPeak as having significant m⁶A enrichment. If a peak was not contained in one region (i.e., if the peak is partly in the CDS and partly in the 3' UTR), it was assigned to the region where more of the peak resided.

Differential m⁶A peak analysis

Regions of differential methylation between two conditions (frequently called “*dTrmt10A*-dependent” or “m⁶A genes”) were found using RADAR (v.0.2.4)⁶⁴ with input and m⁶A pulldown bam files as input, as well as the FlyBase FB2019_05 annotation. All replicates were used for differential peak calling. The minimum cutoff for bin filtering was 15, the cutoff was set as 0.05, and the Beta_cutoff was set as 0.5. Any region with an adjusted *p*-value < 0.05 was retained, and regions with a fold-change < - 1 from the control (KK Control) to the upregulation (UAS-*dTrmt10A*) at basal or heat shock (30 min) conditions were kept as *dTrmt10A*-dependent peaks. All other genes expressed in the brain that did not have *dTrmt10A*-dependent m⁶A were considered as “all other genes.” Full RADAR differential peaks with no cut-off are listed in Supplementary Data 2.

m⁶A metaplots and genome browser visualization

Heatmaps and metagene plots showing the location of m⁶A enrichment on a specific set of genes were constructed with using pheatmaps (v.1.0.12) and meRIPtools (v.0.2.1). Specifically, the exons of all transcripts in each gene were collapsed using the GenomicRanges (v.1.44.0) function reduce⁶⁵. Genes with a 5' UTR or 3' UTR shorter than 30 base pairs, a CDS shorter than 100 bp, or lacking a 5'/3' UTR (i.e., lncRNAs) were not considered in this analysis. For each gene, the 5' UTR and 3' UTR were tiled in 30 evenly spaced bins, and the CDS was tiled in 100 evenly spaced bins. The number of input and m⁶A reads overlapping each bin was calculated and this number was divided by the bin width and library size and a normalization factor of one million to produce a normalized reads per million in each bin. For genome browser snapshots, separated input and m⁶A-IP tracks were visualized. Tracks were made by first converting bam files to bigWig files using deepTools (v.3.5.1)⁶⁶ bamCoverage using CPM normalization, then deepTools bigwigCompare with operation log2.

GO and pathway analysis

GO analysis for genes with *dTrmt10A*-dependent m⁶A was conducted using FlyMine (v.53)⁶⁷. The test correction was set to Holm-Bonferroni with a max *p*-value of 0.05. KEGG^{49,50} pathway analysis was done using the “enrichKEGG” function from ClusterProfiler (v.4.0.5) package in R⁶⁸. A list of all genes with detectable expression was used as background for both GO and pathway analysis.

RNA-seq analysis

Raw paired-end fastqs were processed with TrimGalore (v.0.6.6) (<https://github.com/FelixKrueger/TrimGalore>) with default settings to remove Illumina adapters and mapped using STAR 2.7.3a⁶⁹ to the *Drosophila melanogaster* genome annotation dm6. Unmapped and improperly paired reads were filtered out of aligned bam files. Reads per gene in the FlyBase release 2019_05 were computed using an R script using GenomicRanges (v.1.44.0)⁷⁰ function summarizeOverlaps that counts the number of reads overlapping with the exons of each gene in the default “union” mode. Differential expression analysis was performed using DESeq2 (v.1.32.0)⁷¹, with count files produced by summarizeOverlaps as input. PCA plots were made using the plotPCA function in DESeq2, with variance stabilized counts as the input. MA plots were constructed from the adjusted *p*-values and base-Mean values output from DESeq2, and volcano plots were constructed from adjusted *p*-values and fold changes

reported by DESeq2. Normalized counts produced by DESeq2 were used to show expression levels. Differentially expressed genes were considered to be any gene with a *p*-adjusted values of < 0.05.

Actinomycin assay

Brains from KK Control, UAS-*dTrmt10A*, and *Trmt10A* RNAi adults were dissected and incubated in 250 µl of Schneider's *Drosophila* Medium that was pre-warmed to 25 °C in RNase free 1.5 ml microfuge tubes. 12–15 brains were dissected for each timepoint. 169.5 µg/ml actinomycin D (Sigma-Aldrich, A1410) was added to each sample. Samples were incubated at 25 °C shaking at 300 rpm for 4 h, and mixed by pipetting every 1 h. After the incubation time samples were collected, spun at room temp, washed in cold RNase free PBS, and processed in Trizol. Brain total RNA was collected using trizol/chloroform and Zymo RNA clean and concentrator kit-5 (R1015). RNA was then used for RT-qPCR. 400 ng of RNA is used per cDNA reaction. cDNA is also quantified by Qubit ssDNA Assay (Invitrogen, Q10212) before use in RT-qPCR experiments.

Puromycin assay

Food was made by mixing 600 µM puromycin (Sigma-Aldrich, P8833-100MG) with 2% agar + 5% sucrose. Adult flies were placed onto puromycin food for 24 h. Brains were dissected from flies after 24 h of feeding and samples were processed in for western blot analysis. Protein loading was determined by Ponceau S stain of membrane.

Quantification and statistical analysis

Statistical tests used were performed on GraphPad Prism (v.9), and are indicated in the figure legend. *p*-values of < 0.05 were considered significant. Unpaired two-tailed *t*-tests were used when comparing 2 groups; One-way ANOVA was used when comparing multiple groups followed by Tukey's post-test when each group was compared against every other group, Sidak's post-test when pre-defined groups were compared to each other, or Dunnett's test when comparing to a defined control sample. Two-way ANOVA was used when there were 2 factors in the analysis. One-sided Hypergeometric test was used to compare Venn diagram overlaps.

Salivary gland immunohistochemistry

Third instar larva were dissected in PBST (0.05% Tween 20) and salivary glands were fixed in 2% paraformaldehyde (Electron Microscopy Sciences, #15713) in 45% acetic acid (Alfa Aesar, #36289) for 1 min at room temperature. Fixed salivary glands were loaded in 45% acetic acid on the slide glass and covered with siliconizing reagent (Sigmacote, Sigma-Aldrich, #SL2) coated coverslips to squash polytene chromosomes. Slides were snap frozen with liquid nitrogen and coverslips removed. Samples were blocked with 3% BSA (Sigma, #A7906) solution in PBST for 1 h at room temperature. Primary antibody against HA (Santa cruz, sc-805) and goat anti-rabbit IgG Alexa Fluor488 (Invitrogen, #A11008) were diluted with blocking solution in 1:50 and 1:200 ratio, respectively. VECTASHIELD mounting medium with DAPI (Vector Laboratories, #H-1500) was added at the last step to stain nucleic acids and mount samples. Imaging was conducted on a Leica STELLARIS 5 confocal microscope.

CHIP-WB and RNase treatment

Fly brains (30 brains/sample) were dissected in cold PBS buffer and fixed in 1% formaldehyde (Fisher Scientific, #BP531) for 10 min at room temperature, and washed 3 times with PBS buffer. Fixed brain samples were homogenized in lysis buffer 1 (50 mM HEPES pH7.5, 140 mM NaCl, 1 mM EDTA, 10% Glycerol, 0.5% NP-40, 0.25% Triton X-100), and treated with lysis buffer 2 (10 mM Tris pH8, 200 mM NaCl, 1 mM EDTA, 0.5 mM EGTA), then chromatin samples were collected after sonication in lysis buffer 3 (10 mM Tris pH 8, 100 mM NaCl, 1 mM EDTA, 0.5 mM EGTA, 0.1% Sodium Deoxycholate, 0.5% N-lauroylsarcosine). 10% of chromatin sample was used for input samples. Anti-HA (Santa Cruz, #sc-7392X, 2 µg) and normal mouse IgG (Santa cruz, #sc-2025, 2 µg) antibodies were added to Dynabeads Protein A (Invitrogen, #10002D) and incubated for 6 h at 4 °C. Then applied beads to chromatin samples for overnight incubation at 4 °C. Beads were washed and then denatured with LDS sample buffer (Invitrogen, #NP0007) at 95 °C for 5 min. Beads and supernatant were separated on a magnet stands, and the supernatant was used to perform western blot. For RNase treatment, RNase A/T1 mix (Thermo Scientific, #EN0551) was added to lysis buffer 2, and incubated with brain pellets for 2 h at 4 °C.

Immunoprecipitation with dTrmt10A

To immunoprecipitate dTrmt10A from adult fly heads the Pierce Co-Immunoprecipitation kit (Thermo Scientific, #26149) was utilized according to manufacturer's instructions. 15 µg either anti-HA antibody (mouse, Santa Cruz, #sc-7392X) or mouse IgG (mouse, Santa Cruz, #sc-2025) was immobilized to agarose resin according to kit instructions. Heads of adult male flies expressing UAS-*dTrmt10A*-FLAG-HA with *daGal4* were isolated and homogenized for 1 min on ice in 200 µL of IP Lysis/wash buffer (Thermo Scientific) that was supplemented with cComplete Mini EDTA-free protease inhibitor (Roche, #11836170001). 20 µL of sample was removed for input. Remaining sample lysate was pre-cleared with agarose resin (1 h at 4 °C with gentle rocking). Pre-cleared lysate was incubated with antibody-coupled resin overnight (~ 18 h) at 4 °C with gentle rocking. Agarose resin was then washed three times with IP Lysis/wash buffer supplemented with protease inhibitor (10 min each with rotation at 1000×g, 4 °C). IP samples were eluted in either 50 µL for immunoblotting or 30 µL for mass spec analysis. Samples for immunoblotting were prepared in 4× LDS Sample Buffer (Invitrogen, #NP0007), heat denatured at 90 °C for 6 min and electrophoresed on a 4–12% Bis-Tris gel and transferred to nitrocellulose. dTrmt10A signal was detected using anti-HA-peroxidase antibody (1:500 rat, Roche, #12013819001).

Mass spectrometry analysis of dTrmt10A protein

dTrmt10A was immunoprecipitated from adult fly heads (80 per replicate, $n = 3$ biological replicates per antibody) as described above using anti-HA antibody or mouse IgG as control. Samples were run on NuPAGE™ 10%, Bis-Tris gel for 0.5 cm, and stained using Imperial™ Protein Stain (ThermoFisher, #24615). Mass spectrometry analysis was done by Wistar Proteomics and Metabolomics Facility. The entire stained gel regions were excised, reduced with TCEP, alkylated with iodoacetamide, and digested with trypsin, and tryptic digests were analyzed using a standard 1.5-h LC gradient on the Thermo Q Exactive Plus mass spectrometer. MS data were searched with full tryptic specificity against the UniProt *Drosophila melanogaster* proteome database (7/21/2022) plus the sequence provided (dTrmt10A-HA), and a common contaminant database using MaxQuant 1.6.3.3. Fold change was calculated based on intensity of HA signal to IgG signal, and intensity is the sum of the peptide MS peak intensities for the protein. To calculate the fold change, protein intensity values were processed by: Log2 transformation of the intensity values and replacing missing values (proteins not identified) with the minimum value of the dataset, for comparison between two sample groups, Log2 ratio, Fold change and Student's t -test p -value were calculated using the Log2 imputed intensity, the more stringent q -value (t -test p -value adjusted to account for multiple testing using Benjamini–Hochberg FDR) was also calculated. "High" confident identification of proteins with significant change ("Confident" column) refers to proteins satisfying the 4 criteria: minimum absolute fold change of 2, and q -value < 0.1 , and identified by a minimum of 2 razor + unique peptides in HA-IP group, and detected in at least 2 of the HA-IP replicates. "Medium" confident protein identifications refer to proteins satisfying the 3 criteria: Identified by a minimum of 2 razor + unique peptides in HA-IP group, and detected in at least 2 of the HA-IP replicates, and not detected in any of the IgG-IP replicates.

Data availability

The Raw sequencing data generated in this study have been deposited in the Gene Expression Omnibus GSE229430. Any additional inquiries can be directed to the corresponding author.

Received: 27 June 2023; Accepted: 18 December 2023

Published online: 28 December 2023

References

- Zhao, B. S., Roundtree, I. A. & He, C. Post-transcriptional gene regulation by mRNA modifications. *Nat. Rev. Mol. Cell Biol.* **18**, 31–42 (2017).
- Yang, Y., Hsu, P. J., Chen, Y.-S. & Yang, Y.-G. Dynamic transcriptomic m^6A decoration: Writers, erasers, readers and functions in RNA metabolism. *Cell Res.* **28**, 616–624 (2018).
- Kan, L. *et al.* A neural m^6A /Ythdf pathway is required for learning and memory in *Drosophila*. *Nat. Commun.* **12**, 1458 (2021).
- Widagdo, J., Wong, J.J.-L. & Anggono, V. The m^6A -epitranscriptome in brain plasticity, learning and memory. *Semin. Cell Dev. Biol.* **125**, 110–121 (2022).
- Koranda, J. L. *et al.* Mettl14 is essential for epitranscriptomic regulation of striatal function and learning. *Neuron* **99**, 283–292.e5 (2018).
- Shi, H. *et al.* m^6A facilitates hippocampus-dependent learning and memory through YTHDF1. *Nature* **563**, 249–253 (2018).
- Zhao, B. S. *et al.* m^6A -dependent maternal mRNA clearance facilitates zebrafish maternal-to-zygotic transition. *Nature* **542**, 475–478 (2017).
- Shi, H., Wei, J. & He, C. Where, when and how: Context-dependent functions of RNA methylation writers, readers, and erasers. *Mol. Cell* **74**, 640–650 (2019).
- Cui, Q. *et al.* m^6A RNA methylation regulates the self-renewal and tumorigenesis of glioblastoma stem cells. *Cell Rep.* **18**, 2622–2634 (2017).
- Angelova, M. T. *et al.* The emerging field of epitranscriptomics in neurodevelopmental and neuronal disorders. *Front. Bioeng. Biotechnol.* **6**, 46 (2018).
- Nau, F. The methylation of tRNA. *Biochimie* **58**, 629–645 (1976).
- Pan, T. Modifications and functional genomics of human transfer RNA. *Cell Res.* **28**, 395–404 (2018).
- Cosentino, C. *et al.* Pancreatic β -cell tRNA hypomethylation and fragmentation link TRMT10A deficiency with diabetes. *Nucl. Acids Res.* **46**, 10302–10318 (2018).
- Gillis, D. *et al.* TRMT10A dysfunction is associated with abnormalities in glucose homeostasis, short stature and microcephaly. *J. Med. Genet.* **51**, 581–586 (2014).
- Igoillo-Esteve, M. *et al.* tRNA methyltransferase homolog gene TRMT10A mutation in young onset diabetes and primary microcephaly in humans. *PLoS Genet.* **9**, e1003888 (2013).
- Narayanan, M. *et al.* Case Report: Compound heterozygous nonsense mutations in TRMT10A are associated with microcephaly, delayed development, and periventricular white matter hyperintensities. *F1000Res* **4**, 912 (2015).
- Vilardo, E. *et al.* Functional characterization of the human tRNA methyltransferases TRMT10A and TRMT10B. *Nucl. Acids Res.* **48**, 6157–6169 (2020).
- Hong, J., Xu, K. & Lee, J. H. Biological roles of the RNA m^6A modification and its implications in cancer. *Exp. Mol. Med.* **54**, 1822–1832 (2022).
- Lence, T., Soller, M. & Roignant, J.-Y. A fly view on the roles and mechanisms of the m^6A mRNA modification and its players. *RNA Biol.* **14**, 1232–1240 (2017).
- Engel, M. *et al.* The role of m^6A /m-RNA methylation in stress response regulation. *Neuron* **99**, 389–403.e9 (2018).
- Anders, M. *et al.* Dynamic m^6A methylation facilitates mRNA triaging to stress granules. *Life Sci. Alliance* <https://doi.org/10.26508/lsa.201800113> (2018).
- Weng, Y.-L. *et al.* Epitranscriptomic m^6A regulation of axon regeneration in the adult mammalian nervous system. *Neuron* **97**, 313–325.e6 (2018).
- Hausmann, I. U. *et al.* m^6A potentiates Sxl alternative pre-mRNA splicing for robust *Drosophila* sex determination. *Nature* **540**, 301–304 (2016).
- Bartosovic, M. *et al.* N6-methyladenosine demethylase FTO targets pre-mRNAs and regulates alternative splicing and 3'-end processing. *Nucl. Acids Res.* **45**, 11356–11370 (2017).
- Shi, H. *et al.* YTHDF3 facilitates translation and decay of N6-methyladenosine-modified RNA. *Cell Res.* **27**, 315–328 (2017).
- Meyer, K. D. *et al.* 5' UTR m^6A promotes cap-independent translation. *Cell* **163**, 999–1010 (2015).
- Ontiveros, R. J. *et al.* Coordination of mRNA and tRNA methylations by TRMT10A. *PNAS* **117**, 7782–7791 (2020).

28. Meyer, K. D. *et al.* Comprehensive analysis of mRNA methylation reveals enrichment in 3' UTRs and near stop codons. *Cell* **149**, 1635–1646 (2012).
29. Merkurjev, D. *et al.* Synaptic N6-methyladenosine (m⁶A) epitranscriptome reveals functional partitioning of localized transcripts. *Nat. Neurosci.* **21**, 1004–1014 (2018).
30. Yoon, K.-J. *et al.* Temporal control of mammalian cortical neurogenesis by m⁶A methylation. *Cell* **171**, 877–889.e17 (2017).
31. Edens, B. M. *et al.* FMRP modulates neural differentiation through m⁶A-dependent mRNA nuclear export. *Cell Rep.* **28**, 845–854.e5 (2019).
32. Du, H. *et al.* YTHDF2 destabilizes m⁶A-containing RNA through direct recruitment of the CCR4–NOT deadenylase complex. *Nat. Commun.* **7**, 12626 (2016).
33. Li, M. *et al.* Ythdf2-mediated m⁶A mRNA clearance modulates neural development in mice. *Genome Biol.* **19**, 69 (2018).
34. Haigis, M. C. & Yankner, B. A. The aging stress response. *Mol. Cell* **40**, 333–344 (2010).
35. Kagias, K., Nehammer, C. & Pockock, R. Neuronal responses to physiological stress. *Front. Genet.* **3**, 222 (2012).
36. Vihervaara, A., Duarte, F. M. & Lis, J. T. Molecular mechanisms driving transcriptional stress responses. *Nat. Rev. Genet.* **19**, 385–397 (2018).
37. Zaccara, S. & Jaffrey, S. R. A unified model for the function of YTHDF proteins in regulating m⁶A-modified mRNA. *Cell* **181**, 1582–1595.e18 (2020).
38. Xiang, Y. *et al.* RNA m⁶A methylation regulates the ultraviolet-induced DNA damage response. *Nature* **543**, 573–576 (2017).
39. Knuckles, P. *et al.* RNA fate determination through cotranscriptional adenosine methylation and microprocessor binding. *Nat. Struct. Mol. Biol.* **24**, 561–569 (2017).
40. Ji, Q., Zong, X., Mao, Y. & Qian, S.-B. A heat shock–responsive lncRNA Heat acts as a HSF1-directed transcriptional brake via m⁶A modification. *PNAS* **118**, e2102175118 (2021).
41. Zhou, J. *et al.* Dynamic m⁶A mRNA methylation directs translational control of heat shock response. *Nature* **526**, 591–594 (2015).
42. Bonini, N. M. Chaperoning brain degeneration. *Proc. Natl. Acad. Sci. U.S.A.* **99**(Suppl 4), 16407–16411 (2002).
43. Kan, L. *et al.* The m⁶A pathway facilitates sex determination in *Drosophila*. *Nat. Commun.* **8**, 15737 (2017).
44. Lence, T. *et al.* m⁶A modulates neuronal functions and sex determination in *Drosophila*. *Nature* **540**, 242–247 (2016).
45. Worpenberg, L. *et al.* Ythdf is a N6-methyladenosine reader that modulates Fmr1 target mRNA selection and restricts axonal growth in *Drosophila*. *EMBO J.* **40**, e104975 (2021).
46. Perlegos, A. E., Shields, E. J., Shen, H., Liu, K. F. & Bonini, N. M. Mettl3-dependent m⁶A modification attenuates the brain stress response in *Drosophila*. *Nat. Commun.* **13**, 5387 (2022).
47. Wang, Y. *et al.* Role of Hakai in m⁶A modification pathway in *Drosophila*. *Nat. Commun.* **12**, 2159 (2021).
48. Bawankar, P. *et al.* Hakai is required for stabilization of core components of the m⁶A mRNA methylation machinery. *Nat. Commun.* **12**, 3778 (2021).
49. Kanehisa, M. & Goto, S. KEGG: Kyoto encyclopedia of genes and genomes. *Nucl. Acids Res.* **28**, 27–30 (2000).
50. Kanehisa, M., Furumichi, M., Sato, Y., Kawashima, M. & Ishiguro-Watanabe, M. KEGG for taxonomy-based analysis of pathways and genomes. *Nucl. Acids Res.* **51**, D587–D592 (2023).
51. Akhtar, J. *et al.* m⁶A RNA methylation regulates promoter—Proximal pausing of RNA polymerase II. *Mol. Cell* **81**, 3356–3367.e6 (2021).
52. Liu, J. *et al.* N6-methyladenosine of chromosome-associated regulatory RNA regulates chromatin state and transcription. *Science* **367**, 580–586 (2020).
53. Xu, W. *et al.* METTL3 regulates heterochromatin in mouse embryonic stem cells. *Nature* **591**, 317–321 (2021).
54. Hilgers, V., Lemke, S. B. & Levine, M. ELAV mediates 3' UTR extension in the *Drosophila* nervous system. *Genes Dev.* **26**, 2259–2264 (2012).
55. Wei, L. *et al.* Overlapping activities of ELAV/Hu family RNA binding proteins specify the extended neuronal 3' UTR landscape in *Drosophila*. *Mol. Cell* **80**, 140–155.e6 (2020).
56. Fu, Y. *et al.* FTO-mediated formation of N6-hydroxymethyladenosine and N6-formyladenosine in mammalian RNA. *Nat. Commun.* **4**, 1798 (2013).
57. Zheng, H., Zhao, Y., Zhou, H., Tang, Y. & Xie, Z. The comprehensive analysis of m⁶A-associated Anoikis genes in low-grade gliomas. *Brain Sci.* **13**, 1311 (2023).
58. Batista, P. J. *et al.* m⁶A RNA modification controls cell fate transition in mammalian embryonic stem cells. *Cell Stem Cell* **15**, 707–719 (2014).
59. Ostrowski, L. A., Hall, A. C. & Mekhail, K. Ataxin-2: From RNA control to human health and disease. *Genes (Basel)* **8**, 157 (2017).
60. Perkins, L. A. *et al.* The transgenic RNAi project at Harvard Medical School: Resources and validation. *Genetics* **201**, 843–852 (2015).
61. Dietzl, G. *et al.* A genome-wide transgenic RNAi library for conditional gene inactivation in *Drosophila*. *Nature* **448**, 151–156 (2007).
62. Kennerdell, J. R., Liu, N. & Bonini, N. M. MiR-34 inhibits polycomb repressive complex 2 to modulate chaperone expression and promote healthy brain aging. *Nat. Commun.* **9**, 4188 (2018).
63. Cui, X., Meng, J., Zhang, S., Chen, Y. & Huang, Y. A novel algorithm for calling mRNA m⁶A peaks by modeling biological variances in MeRIP-seq data. *Bioinformatics* **32**, i378–i385 (2016).
64. Zhang, Z. *et al.* RADAR: Differential analysis of MeRIP-seq data with a random effect model. *Genome Biol.* **20**, 294 (2019).
65. Zhang, Z. *et al.* Genetic analyses support the contribution of mRNA N6-methyladenosine (m⁶A) modification to human disease heritability. *Nat. Genetics* **52**, 939–949 (2020).
66. Ramirez, F. *et al.* deepTools2: A next generation web server for deep-sequencing data analysis. *Nucl. Acids Res.* **44**, W160–W165 (2016).
67. Smith, R. N. *et al.* InterMine: A flexible data warehouse system for the integration and analysis of heterogeneous biological data. *Bioinformatics* **28**, 3163–3165 (2012).
68. Yu, G., Wang, L.-G., Han, Y. & He, Q.-Y. clusterProfiler: An R package for comparing biological themes among gene clusters. *OMICS* **16**, 284–287 (2012).
69. Dobin, A. *et al.* STAR: Ultrafast universal RNA-seq aligner. *Bioinformatics* **29**, 15–21 (2013).
70. Lawrence, M. *et al.* Software for computing and annotating genomic ranges. *PLoS Comput. Biol.* **9**, e1003118 (2013).
71. Love, M. I., Huber, W. & Anders, S. Moderated estimation of fold change and dispersion for RNA-seq data with DESeq2. *Genome Biol.* **15**, 550 (2014).

Acknowledgements

We thank the *Drosophila* Genomics Resource Center (NIH grant 2P40OD010949), the Bloomington *Drosophila* Stock Center (NIH P40OD018537) and the Transgenic RNAi Project (TRiP) at Harvard Medical School (NIH/NIGMS R01-GM084947). We thank the Proteomics and Metabolomics Facility at The Wistar Institute. This work was supported by T32-GM007229 and F31-AG063470 (to AEP), R35-GM133721 (to KFL) and R35-NS097275 (to NMB).

Author contributions

A.E.P. conceived, designed, and performed experiments, statistical analysis, bioinformatic analysis, and analyzed data. X.Q. performed chromatin experiments. K.M.D performed immunoprecipitations and assisted in experiments. E.J.S. designed bioinformatic pipeline. H.S. and H.E. performed mass spec experiments. K.F.L. supervised research and analyzed data. N.M.B. conceived, designed experiments, analyzed data, and supervised the research. K.F.L and H.S. gave input and edited the manuscript. A.E.P and N.M.B. wrote the manuscript.

Competing interests

The authors declare no competing interests.

Additional information

Supplementary Information The online version contains supplementary material available at <https://doi.org/10.1038/s41598-023-50272-4>.

Correspondence and requests for materials should be addressed to N.M.B.

Reprints and permissions information is available at www.nature.com/reprints.

Publisher's note Springer Nature remains neutral with regard to jurisdictional claims in published maps and institutional affiliations.



Open Access This article is licensed under a Creative Commons Attribution 4.0 International License, which permits use, sharing, adaptation, distribution and reproduction in any medium or format, as long as you give appropriate credit to the original author(s) and the source, provide a link to the Creative Commons licence, and indicate if changes were made. The images or other third party material in this article are included in the article's Creative Commons licence, unless indicated otherwise in a credit line to the material. If material is not included in the article's Creative Commons licence and your intended use is not permitted by statutory regulation or exceeds the permitted use, you will need to obtain permission directly from the copyright holder. To view a copy of this licence, visit <http://creativecommons.org/licenses/by/4.0/>.

© The Author(s) 2023